Admittance of Irises in Coaxial and Circular Waveguides for TE_{11}-Mode Excitation

GRAEME L. JAMES, SENIOR MEMBER, IEEE

Abstract—**The admittance of irises in both coaxial and circular waveguides is deduced from a mode-matching technique. Design data for the effective admittance to TE_{11}-mode excitation are given for a range of waveguide and iris dimensions.**

I. Introduction

CIRCULARLY SYMMETRIC irises in circular and coaxial waveguides are of considerable use in matching numerous waveguide devices. However, there is a lack of readily available data on the admittance of circular irises in waveguides. The most extensive data are to be found in [1], where the admittance of an iris in circular waveguide for TE_{11}-mode excitation and in a coaxial waveguide for TEM-mode excitation is given. However, there appear to be little or no published data for irises in coaxial waveguides for TE_{11}-mode excitation. Such data are required in matching devices such as coaxial waveguide radiators.

Fig. 1 shows the types of irises possible in coaxial and circular waveguides. In this paper, we derive the admittance characteristics of these irises to the TE_{11} mode using an accurate mode-matching technique. A short description of the method is given in the following section. Using this method, we have produced design data, given in Section III, for a range of waveguide and iris dimensions.

II. Outline of the Theoretical Analysis

In solving for the admittance of the four irises given in Fig. 1, we use the general waveguide model shown in Fig. 2. Since the problem possesses symmetry, we only require the solution for a single waveguide junction. Specifically, we need the scattering matrix for the section of waveguide from $z = 0$ to $z = t/2$. We use the analytical method given in [2], where the junction between two circular waveguides was considered (the special case of $a_{\mathrm{I}} = a_{\mathrm{II}} = 0$). The same general analysis applies here, the only change being the solution of the integrals coupling the transverse fields [2, eq. (4)]. In the present application, the coupling is determined at the junction of the two coaxial waveguides, as shown in Fig. 2. To solve for the admittance of the iris for TE_{11}-mode excitation, we require the complex reflection coefficient Γ of this mode at $z = 0$ (or $z = t$). For unit strength TE_{11}-mode excitation, this is given directly (using the notation in [2]) by the first element in the overall scattering matrix term $\underline{S}_{11}^{0}$ which results from cascading the scattering matrix for $z = 0$ to $z = t/2$ with its reverse configuration. The solution is given in the Appendix, together with the field-coupling integrals for the coaxial waveguide case. In the input waveguide, we took up to 20 modes to ensure adequate convergence of the solution.

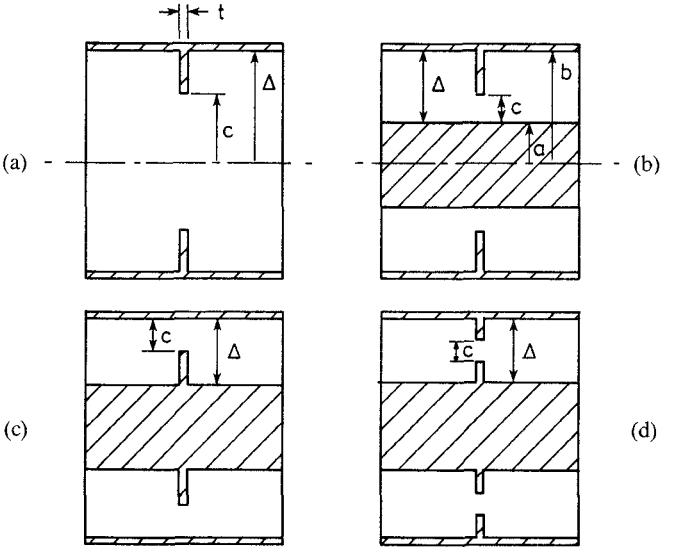

Fig. 1. Various circular iris configurations in coaxial and circular waveguides.

Once the reflection coefficient Γ is known, the normalized admittance of the iris is readily obtained. The effective shunt conductance G and susceptance B of the iris as seen from either $z = 0$ or $z = t$ are obtained from [1] as

$$G/Y_0 = (1 - |\Gamma|^2)/(1 + 2|\Gamma|\cos(\arg\Gamma) + |\Gamma|^2)$$

$$B/Y_0 = -2|\Gamma|\sin(\arg\Gamma)/(1 + 2|\Gamma|\cos(\arg\Gamma) + |\Gamma|^2)$$

where Y_0 is the characteristic admittance of the waveguide of region I in Fig. 2.

In [1], irises of finite thickness are represented by a T-junction of equivalent susceptances or reactances. However, we have chosen to use an effective shunt admittance, since it is easier to apply in practice when using irises to match waveguide devices with the Smith Chart.

Manuscript received August 9, 1986; revised November 28, 1986.
The author is with the Division of Radiophysics, CSIRO, Epping, NSW, Australia 2121.
IEEE Log Number 8613290.

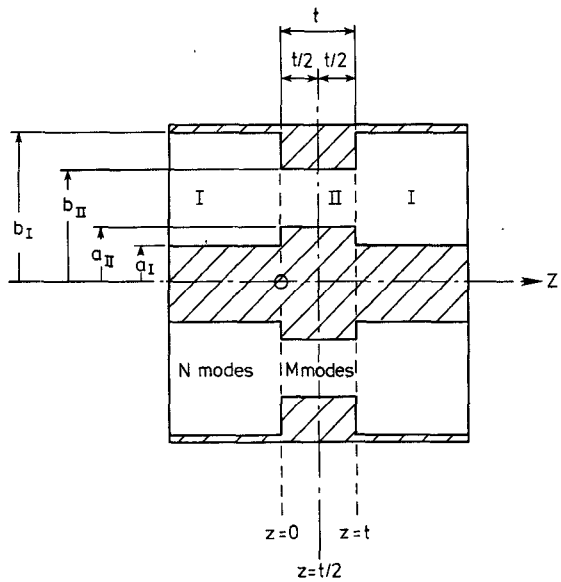

Fig. 2. Cross-section view of the model used to analyze the iris admittance.

III. Results

In the various configurations shown in Fig. 1, there are a large number of possible iris dimensions. To limit our data presentation to manageable proportions, we found that the configuration in Fig. 1(d) offered little advantage over that of Fig. 1(b) and (c); hence, we present data for the first three cases of Fig. 1 only.

The admittance of the iris can be quite sensitive to its thickness t. This is demonstrated by the example in Fig. 3. In practice, t should not be too large but the iris must nevertheless be of sufficient thickness to be mechanically stable. With this in mind and to reduce the number of variables as much as possible, our subsequent results (Figs. 4–10) are restricted to irises with the ratio $t/b = 0.075$. The admittance is plotted against the ratio c/Δ (in the range 0.05 to 0.95) for a range of $k\Delta$ values. This range is restricted to values below the cutoff number of the TM_{11} mode—the first higher order mode than can be excited by the iris. (Note that, since the iris is symmetrical, neither the TM_{01} mode in circular waveguide nor the TEM in coaxial waveguide can be excited by the iris.) To permit reasonable interpolation between the given curves, we have presented results for a/b values, beginning with 0.0 (the circular waveguide case of Fig. 1(a)) in Fig. 4, through 0.1, 0.3, 0.5, and 0.7 in Figs. 5–9. These last five figures are for the configurations shown in Fig. 1(b) and (c). Note that there is considerably less variation in admittance for the configuration of Fig. 1(c) than for Fig. 1(b). Further, it is seen that both positive and negative values of admittance are possible for the irises of Fig. 1(a) and (b), but for the iris of Fig. 1(c) only positive values of admittance occur.

As a check on the accuracy of the numerical predictions, we have compared our results with measured data for the circular waveguide given in [1] and found very good agreement. Further, we have measured the reflection coefficient of irises in coaxial waveguides and found the results to compare well with the theoretical predictions. This is demonstrated by the example given in Fig. 10. Finally, using the data given in Figs. 5–9, we have presented in [3] a theoretical prediction for the matching of a coaxial radiator which agrees closely with measured data.

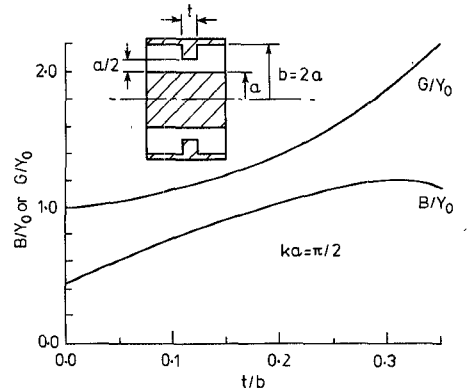

Fig. 3. The effect of iris thickness on the admittance when $b = 2a$ and $c = a/2$.

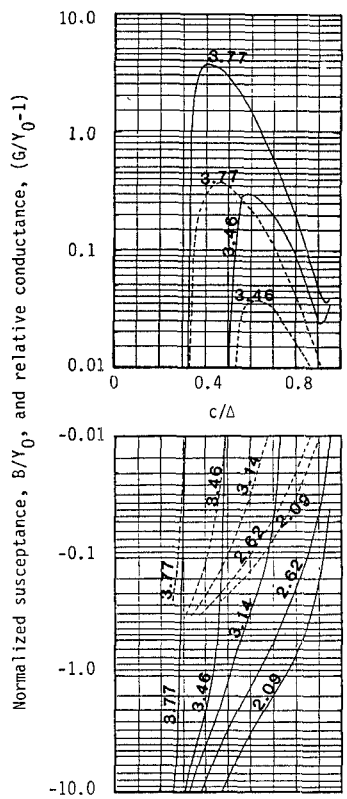

Fig. 4. Admittance of an iris (with $t/b = 0.075$) in a circular waveguide as a function of c/Δ for various values of $k\Delta$. Full line indicates normalized susceptance B/Y_0, and dashed line, relative conductance $(G/Y_0 - 1)$.

Appendix

The overall scattering matrix term $\underline{S}_{11}^0$ for the cascaded waveguide section from $z = 0$ to $z = t$ in Fig. 2 can be readily deduced from the method described in [2]. Taking N modes in region I and M modes in region II, where $N/M = (b_I - a_I)/(b_{II} - a_{II})$ to the nearest rational num-

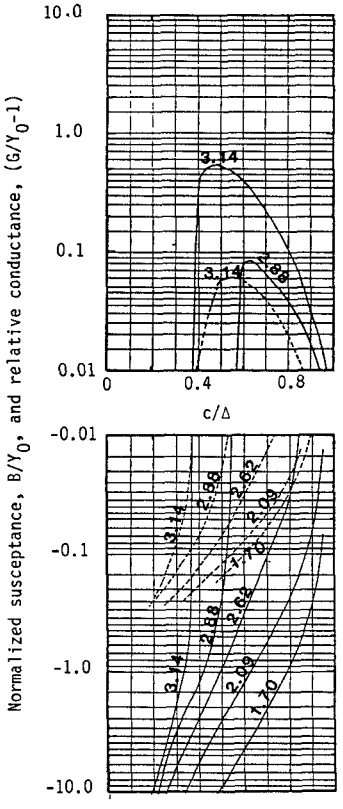

Fig. 5. Admittance of an iris in a coaxial waveguide with the configuration of Fig. 1(b) for various values of $k\Delta$ for $a/b = 0.1$ and $t/b = 0.075$ (key as in Fig. 4).

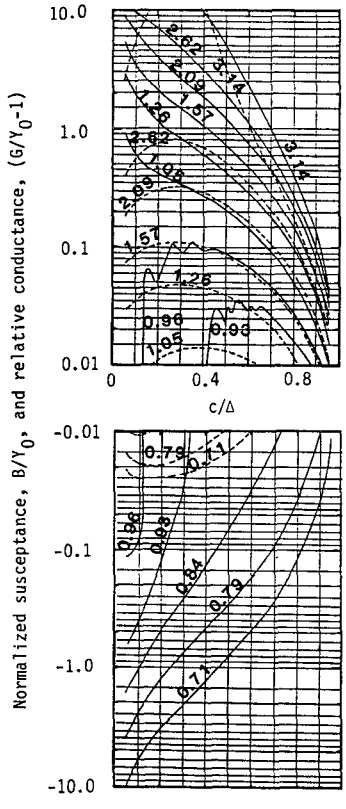

Fig. 7. Admittance of an iris in a coaxial waveguide with the configuration of Fig 1(b) for various values of $k\Delta$ for $a/b = 0.5$ and $t/b = 0.075$ (key as in Fig. 4).

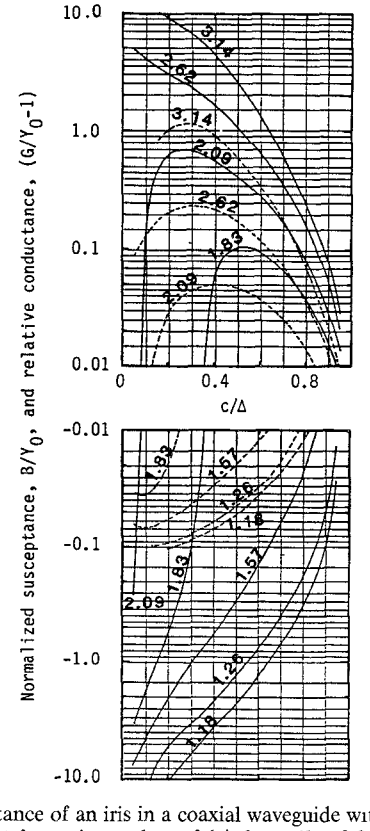

Fig. 6. Admittance of an iris in a coaxial waveguide with the configuration of Fig. 1(b) for various values of $k\Delta$ for $a/b = 0.3$ and $t/b = 0.075$ (key as in Fig. 4).

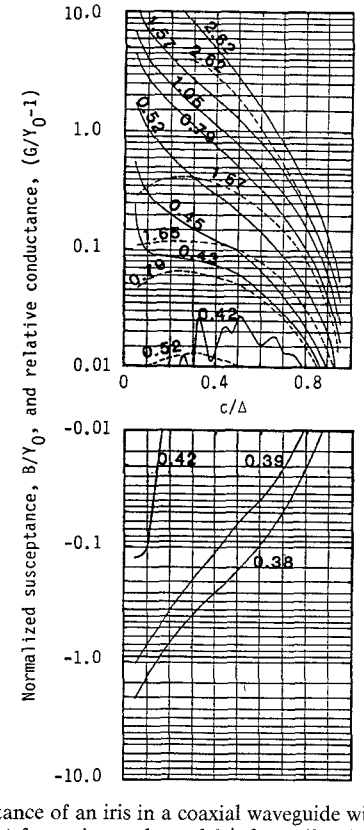

Fig. 8. Admittance of an iris in a coaxial waveguide with the configuration of Fig. 1(b) for various values of $k\Delta$ for $a/b = 0.7$ and $t/b = 0.75$ (key as in Fig. 4).

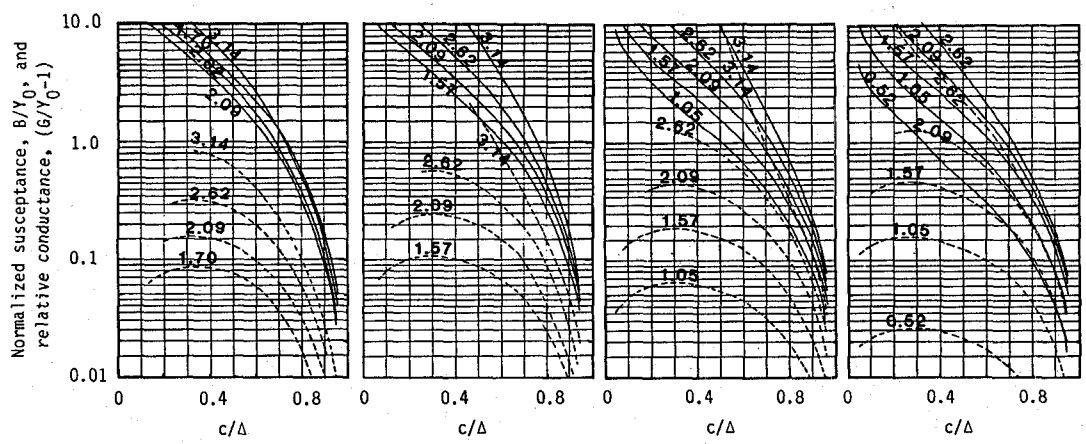

Fig. 9. Admittance of an iris in a coaxial waveguide with the configuration of Fig. 1(c) for various values of $k\Delta$ for $a/b = 0.1$, 0.3, 0.5, and 0.7 and $t/b = 0.075$ (key as in Fig. 4).

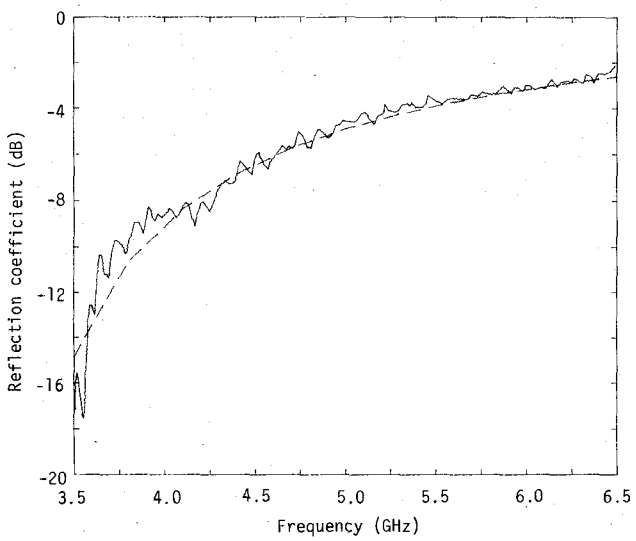

Fig. 10. Measured and predicted values of the reflection coefficient of an iris in a coaxial waveguide with the configuration of Fig. 1(b); $a/b = 0.533$, $c/\Delta = 0.246$, $t/b = 0.075$, where $b = 27$ mm. Full line indicates measured values, and dashed line, predicted.

ber, we can write $\underline{S}_{11}^0$ as

$$\underline{S}_{11}^0 = \underline{S}_{21}\underline{V}\left[\left(\underline{V}\underline{S}_{11}\underline{V}\right)^{-1} - \left(\underline{V}\underline{S}_{11}\underline{V}\right)\right]^{-1}\underline{V}\underline{S}_{12} + \underline{S}_{22}$$

where $\underline{V}$ is an $M \times M$ diagonal matrix with elements $V_{mm} = \exp(-\gamma_m t/2)$, γ_m being the propagation constant of the mth mode in the coaxial waveguide of region II. $\underline{S}_{11}$, $\underline{S}_{12}$, $\underline{S}_{21}$, and $\underline{S}_{22}$ are given by [2, eq. (6)], where the elements P_{mn}, Q_{nn}, and R_{mm} are given—after evaluating the integrals of [2, eq. (4)] for the general coaxial waveguide junction of Fig. 2—by the following expressions:

$$P_{mn} = \frac{\pi}{k\beta_{\mathrm{I}}}\frac{\sqrt{k^2-\beta_{\mathrm{I}}^2}}{\beta_{\mathrm{II}}^2-\beta_{\mathrm{I}}^2}\left[\beta_{\mathrm{II}}b_{\mathrm{II}}H_{\mathrm{II}}(b_{\mathrm{II}})H_{\mathrm{I}}'(b_{\mathrm{II}}) - \frac{2}{\pi}H_{\mathrm{I}}'(a_{\mathrm{II}})\right], \qquad m,n \text{ odd}$$

$$= \frac{\pi}{k}\frac{\alpha_{\mathrm{I}}}{\alpha_{\mathrm{II}}}\frac{\sqrt{k^2-\alpha_{\mathrm{II}}^2}}{\alpha_{\mathrm{II}}^2-\alpha_{\mathrm{I}}^2}\left[b_{\mathrm{II}}K_{\mathrm{II}}(b_{\mathrm{II}})G_{\mathrm{I}}(b_{\mathrm{II}}) - \frac{2}{\pi}G_{\mathrm{I}}(a_{\mathrm{II}})\right], \qquad m,n \text{ even}$$

$$= \frac{\pi}{\alpha_{\mathrm{I}}\beta_{\mathrm{II}}}\left[G_{\mathrm{I}}(b_{\mathrm{II}})H_{\mathrm{II}}(b_{\mathrm{II}}) - \frac{2}{\pi a_{\mathrm{II}}\beta_{\mathrm{II}}}G_{\mathrm{I}}(a_{\mathrm{II}})\right], \qquad m \text{ odd}, n \text{ even}$$

$$= 0, \qquad m \text{ even}, n \text{ odd}$$

$$Q_{nn} = \frac{\pi}{2k}\frac{\sqrt{k^2-\beta_{\mathrm{I}}^2}}{\beta_{\mathrm{I}}^2}\left\{H_{\mathrm{I}}^2(b_{\mathrm{I}})\left(\beta_{\mathrm{I}}^2b_{\mathrm{I}}^2-1\right) - \left(\frac{2}{\pi\beta_{\mathrm{I}}a_{\mathrm{I}}}\right)^2\left(\beta_{\mathrm{I}}^2a_{\mathrm{I}}^2-1\right)\right\}, \qquad n \text{ odd}$$

$$= \frac{\pi}{2k}\frac{\sqrt{k^2-\alpha_{\mathrm{I}}^2}}{\alpha_{\mathrm{I}}^2}\left\{\left[\alpha_{\mathrm{I}}b_{\mathrm{I}}K_{\mathrm{I}}(b_{\mathrm{I}})\right]^2 - \frac{4}{\pi^2}\right\}, \qquad n \text{ even}$$

$$R_{mm} = \frac{\pi}{2k}\frac{\sqrt{k^2-\beta_{\mathrm{II}}^2}}{\beta_{\mathrm{II}}^2}\left\{H_{\mathrm{II}}^2(b_{\mathrm{II}})\left(\beta_{\mathrm{II}}^2b_{\mathrm{II}}^2-1\right) - \left(\frac{2}{\pi\beta_{\mathrm{II}}a_{\mathrm{II}}}\right)^2\left(\beta_{\mathrm{II}}^2a_{\mathrm{II}}^2-1\right)\right\}, \qquad m \text{ odd}$$

$$= \frac{\pi}{2k}\frac{\sqrt{k^2-\alpha_{\mathrm{II}}^2}}{\alpha_{\mathrm{II}}^2}\left\{\left[\alpha_{\mathrm{II}}b_{\mathrm{II}}K_{\mathrm{II}}(b_{\mathrm{II}})\right]^2 - \frac{4}{\pi^2}\right\}, \qquad m \text{ even}$$

where

$$G_{\mathrm{I,II}}(x) = J_1(\alpha_{\mathrm{I,II}}x)Y_1(\alpha_{\mathrm{I,II}}a_{\mathrm{I,II}}) - J_1(\alpha_{\mathrm{I,II}}a_{\mathrm{I,II}})Y_1(\alpha_{\mathrm{I,II}}x)$$

$$H_{\mathrm{I,II}}(x) = J_1(\beta_{\mathrm{I,II}}x)Y_1'(\beta_{\mathrm{I,II}}a_{\mathrm{I,II}}) - J_1'(\beta_{\mathrm{I,II}}a_{\mathrm{I,II}})Y_1(\beta_{\mathrm{I,II}}x)$$

$$K_{\mathrm{I,II}}(x) = J_1(\alpha_{\mathrm{I,II}}a_{\mathrm{I,II}})Y_0(\alpha_{\mathrm{I,II}}x) - Y_1(\alpha_{\mathrm{I,II}}a_{\mathrm{I,II}})J_0(\alpha_{\mathrm{I,II}}x)$$

and $\alpha_{I,II}, \beta_{I,II}$ are the roots of

$$G_{I,II}(b_{I,II}) = 0, H'_{I,II}(b_{I,II}) = 0.$$

ACKNOWLEDGMENT

The author is indebted to S. J. Skinner for the measured results.

REFERENCES

[1] N. Marcuvitz, *Waveguide Handbook* (Radiation Laboratory Series, vol. 10). New York: McGraw-Hill, 1951.

[2] G. L. James, "Analysis and design of TE_{11}-to-HE_{11} corrugated cylindrical waveguide mode converters," *IEEE Trans. Microwave Theory Tech.*, vol. MTT-29, pp. 1059–1066, 1981.

[3] T. S. Bird, G. L. James, and S. J. Skinner, "Input mismatch of TE_{11} mode coaxial waveguide feeds," *IEEE Trans. Antennas Propagat.*, vol. AP-34, pp. 1030–1033, 1986.

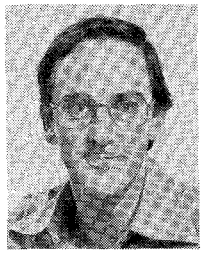

Graeme L. James (SM'84) was born in Dunedin, New Zealand, in 1945. He received the B.E. and Ph.D. degrees in electrical engineering from the University of Canterbury, Christchurch, New Zealand, in 1970 and 1973, respectively. In 1984, he was awarded the D.Sc. degree from the same university.

Between 1973 and 1976, he was a Postdoctoral Fellow with the Department of Electrical and Electronic Engineering, Queen Mary College, London, England, where he was involved in a number of projects concerned with electromagnetic scattering and diffraction. Since June 1976, he has been with the Commonwealth Scientific and Industrial Research Organization Division of Radiophysics in Sydney, where he has been mainly concerned with research into high-performance microwave antennas for both radio astronomy and satellite communications.

Dr. James is a Fellow of the Institute of Electrical Engineeers, London.